

# Planetesimal Formation in Zonal Flows Arising in Magneto-Rotationally-Unstable Protoplanetary Disks

Karsten Dittrich<sup>1</sup>, Hubert Klahr<sup>1</sup> and Anders Johansen<sup>2</sup>

<sup>1</sup>Max-Planck-Institut für Astronomie,  
Königstuhl 17, 69117 Heidelberg, Germany  
email: dittrich@mpia.de, klahr@mpia.de

<sup>2</sup>Lund Observatory, Department of Astronomy and Theoretical Physics,  
Box 43, 221 00 Lund, Sweden  
email: anders@astro.lu.se

**Abstract.** Recent simulations show long-lived sub- and super-Keplerian flows in protoplanetary disks. These so-called zonal flows are found in local as well as global simulations of magneto-rotationally unstable disks. We investigate the strength and life-time of the resulting long-lived gas over- and under-densities as well as particle concentrations function of the azimuthal and radial size of the local shearing box. Changes in the azimuthal extent do not affect the zonal flow features. However, strength and life-time of zonal flows increase with increasing radial box sizes. Our simulations show indications, and support earlier results, that zonal flows have a natural length scale of approximately 5 pressure scale heights. For the first time, the reaction of dust particles in boxes with zonal flows are studied. We show that particles of some centimeters in size reach a hundred-fold higher density than initially, without any self-gravitating forces acting on the point masses. We further investigate collision velocities of dust grains in a turbulent medium.

**Keywords.** Magnetohydrodynamics (MHD) - Planets and satellites: formation - Protoplanetary disks

---

## 1. Introduction

Turbulence in protoplanetary disks around young stars is a promising scenario for rapid planetesimal formation (Johansen *et al.* 2007). Shearing box simulations (Brandenburg *et al.* 1995) are a powerful tool for analyzing the magneto-rotational instability (MRI, Balbus & Hawley 1991, Balbus & Hawley 1998) as a source of turbulence. These simulations consider a local, co-rotating box, representing a small part of a Keplerian disk. Johansen *et al.* (2009a) reported long-lived axisymmetric sub- and super-Keplerian flows, zonal flows, in shearing box simulations of turbulence caused by the MRI. These zonal flows have been seen in several other local (Fromang & Stone 2009, Stone & Gardiner 2010) and global (Lyra *et al.* 2008, Flock *et al.* 2011) simulations.

Zonal flows are a product of large-scale variation in the magnetic field that transport momentum differentially, creating regions of slightly faster and slightly slower rotating gas. Large-scale pressure bumps are excited through geostrophic balance. This creates long-lived over-densities that potentially trap dust particles. A more thorough description of zonal flows and their creation is found in Johansen (2009). Johansen *et al.* (2009a) found zonal flows always populating the largest radial mode available in the local box approximation. Their largest box was simulating 10.56 pressure scale heights.

This IAUS proceeding is based on Dittrich *et al.* (2013). In this work we consider even larger physical extents for zonal flow structures. This gives us the opportunity to measure physical properties such as size and life-time independent of the simulated domain. Further, we investigate properties of the zonal flows in radially and azimuthally stretched boxes. We alter the radial and azimuthal domain up to  $\sim 20$  gas pressure scale heights. Additionally, we study the behavior of dust in zonal flows. Dust trapping was studied in a 1D radial model since Whipple (1972). Pinilla *et al.* (2012) invoked zonal flows as a possibility to explain the sub-millimeter and millimeter-sized particles observed in protoplanetary disks.

## 2. Simulation Setup

We use the Pencil Code<sup>†</sup>, a 6<sup>th</sup> order spatial and 3<sup>rd</sup> order temporal finite difference code, for our simulations. We simulated the standard ideal MHD equations in a local shearing box with vertical stratification. The simulation boxes are centered at an arbitrary distance  $r$  to the star. The radial direction is denoted by  $x$ , the azimuthal direction by  $y$ , and the vertical direction by  $z$ . The Keplerian frequency is  $\Omega$ . We included dust particle dynamics, without back-reaction to the gas and without self-gravity. The full equations can be found in Dittrich *et al.* (2013).

## 3. Results

Dust capture in zonal flows. Particle accumulations and planetesimal formation can occur in clumps and filaments of the over-densities in the dust. If the dust density exceeds the Roche density, a clump is gravitationally bound against shear. The Roche density can be approximated (Kopal 1989) by

$$\rho_{\text{Roche}}(R = 5 \text{ AU}) = \frac{9}{4\pi} \frac{\Omega^2}{G(R = 5 \text{ AU})} \sim 100\rho(R = 5 \text{ AU}), \quad (3.1)$$

for a MMSN.  $G$  is the gravitational constant. In our simulations we do not include gravitational interaction between the particles. Thus, we only study the passively developed over-densities of the dust to see when and whether over-densities sufficient for the streaming instability can be reached. By not having explicit feedback one can retroactively study the concentration factor for various initial dust-to-gas ratios. Simulations including feedback will have to be done in future studies.

Particles in zonal flows. In the upper right panel of Fig. 1, the azimuthal gas velocity development of run *XXL* is shown, over-plotted with the position of the most massive clump for each time step. The azimuthal gas velocity coincides with the derivative of the gas density, but it is much easier to interpret. The speckled structure of the derivatives comes due to the high power in the smaller scales. However, the large-scale structure is still visible and the geostrophic correlation between the structures of  $u_y(x, t)$  and  $d/dx[\rho(x, t)]$  is directly observed. Since they have the same large-scale structure, the particle position is much easier interpreted at the azimuthal gas velocity plot than on the derivative plot. Sometimes the radial displacement from one orbit to the next is too large to be explained by radial drift. That happens when another clumps becomes more massive than the previous one. These particles accumulate in regions with high azimuthal gas velocities (see upper right panel in Fig. 1). The only time when this is not true is at times from 80 to 100 local orbits. In this period an inwards-drifting clump

<sup>†</sup> Details on the Pencil Code at <http://www.nordita.org/software/pencil-code/>.

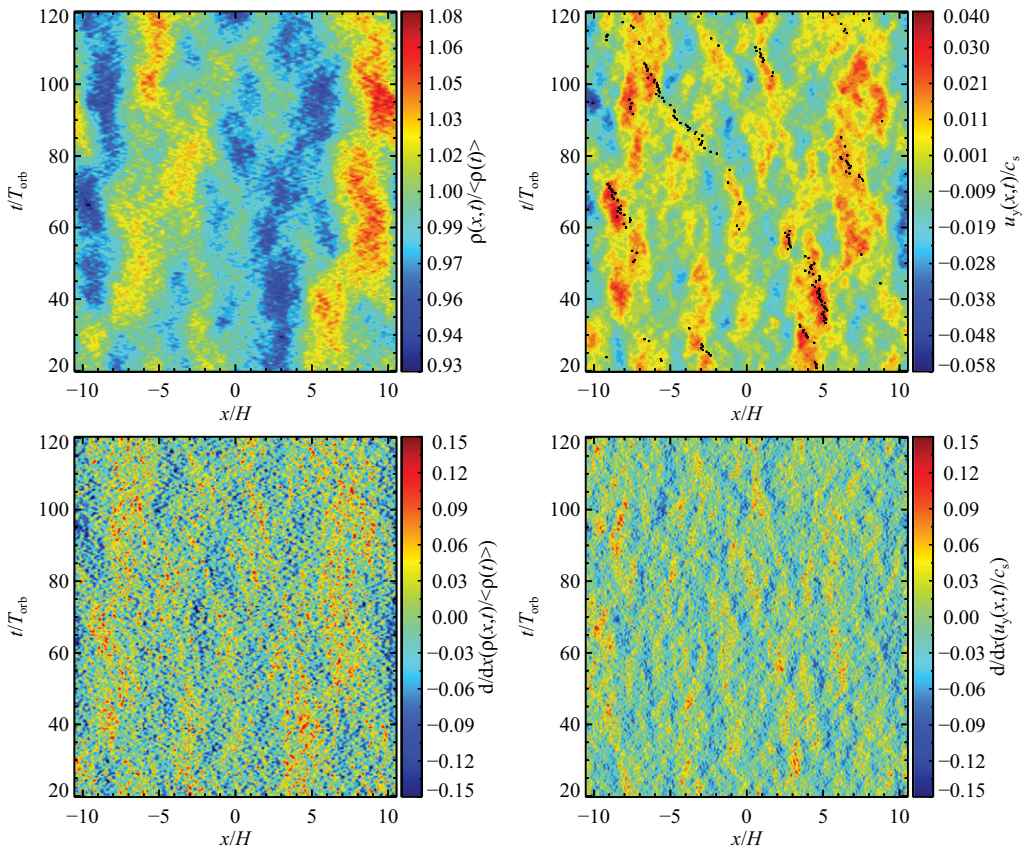


**Figure 1.** The top panels show the gas density evolution and the evolution of the azimuthal gas velocity of run *XXL*, our largest simulation. The bottom row shows the radial derivative of these quantities. The derivatives are very speckled, since small scale fluctuations give stronger amplitudes to the derivatives. However, the underlying large scale structure is still visible. The azimuthal gas velocity follows the radial gas density gradient, as expected for a geostrophic balance. Hence, it is possible to interpret the radial derivative of the azimuthal gas velocity as the second derivative of the gas density. In the upper right panel, the black dots represent the position of the most massive particle clump in the simulation at each time. The sudden large changes in the radial position are explained by another clump at a different location becoming more massive than the previous clump. It is clearly shown that particles get trapped in regions of positive zonal flow downstream of pressure bumps.

stayed coherent during the time of its drift. The drift velocity of the most massive particle clump is indirectly encrypted in this plot. Particles are drifting much slower when they are trapped by a pressure gradient. As all particles drift inwards this leads to accumulation of particles in regions where the perturbed pressure gradient is positive.

In isothermal geostrophic balance,  $2\rho\Omega u_y = c_s^2 \partial\rho/\partial x$ , the azimuthal gas velocity follows the radial density gradient. That this is true for large scales as shown in Fig. 2. The upper left panel shows the evolution of the azimuthally and vertically averaged azimuthal component of the gas velocity. Over-plotted are the locations of the maxima in the dust density. In the upper right panel the dust density evolution of the same run *L* is plotted. In comparing the location and times of the maxima and minima on these two plots, one clearly sees that maxima in the dust density occur often at times and locations where one finds maxima in the gas velocity. Without radial drift particles would concentrate where

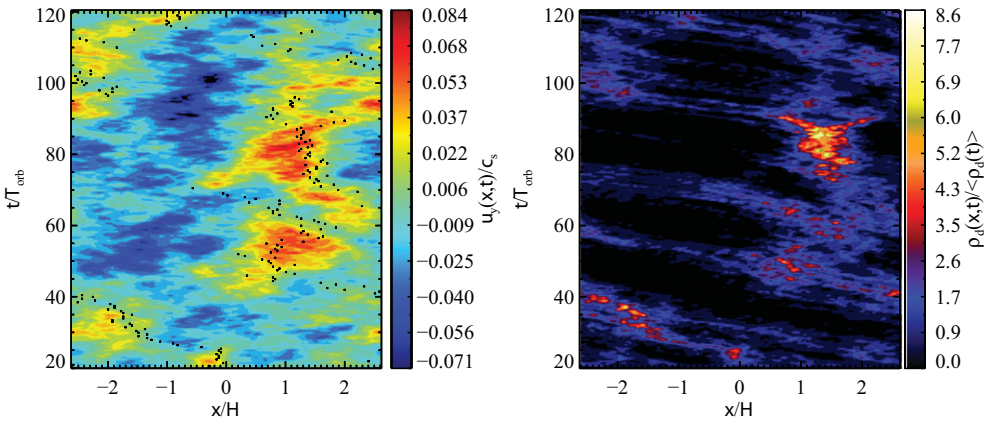


**Figure 2.** The evolution of the azimuthal gas velocity (left) and the dust density (right) evolution of run *L* respectively. The quantities are averaged in vertical and azimuthal direction and plotted in radial direction over time. The black dots in the left panel show the position of the highest dust density at each orbit. This shows that the over-densities of the dust often appears at places and times where the azimuthal gas velocity is high. This relation shows that the zonal flows accumulate dust and are a possible venue of planetesimal formation.

$u_y = 0$ , i.e., between the sub- and super-Keplerian flow. Due to the radial drift particles accumulate slightly downstream at the formed pressure bumps. Those happen to be at the maxima of the azimuthal gas velocity. With the geostrophic balance, high azimuthal velocities are also regions of a high density gradient. These plots prove that the particles in the simulations are trapped by the long lived pressure gradients that occur due to stable zonal flows.

If the dust-to-gas ratio increases to values larger than unity, the streaming instability (Johansen & Youdin 2007, Youdin & Johansen 2007) is triggered. This increases the dust density further on timescales shorter than an orbital period. To follow the streaming instability development, the back-reaction of the dust particles to the gas phase must be considered in future numerical simulation. This effect was neglected in this set of simulations. Otherwise the initial dust-to-gas ratio would have been an additional free parameter to be studied.

*Different particle sizes.* So far we did only consider simulations with one particle species, i.e.,  $St = \tau_f \Omega = 1$ . We take the simulation size that simulates one fully extended zonal flow and investigate different particle species. The particle sizes range from  $St = 0.01$  to  $St = 100$ . We choose run *L* with the dimensions  $5.28H \times 5.28H \times 2.64H$  as simulation size for the last simulation. We further almost doubled<sup>†</sup> the resolution. This was done to verify that dust capture is independent of the chosen resolution.

Fig. 3 shows the total particles over-density normalized to the initial particle number density. Since this simulation did not include the back-reaction from the dust to the gas, we could study the behavior of 12 different particle sizes, i.e., Stokes numbers. The highest concentrations were reached for particles of sizes  $St = 0.75 \dots 5$ , as expected.  $St = 0.1$  particles get concentrated well into the streaming instability regime. Future studies including the back-reaction and self-gravity will test further growth of the formed clumps.

<sup>†</sup> We increased the resolution from 36 grid cells /  $1.32H$  to  $64/1.32H$ .

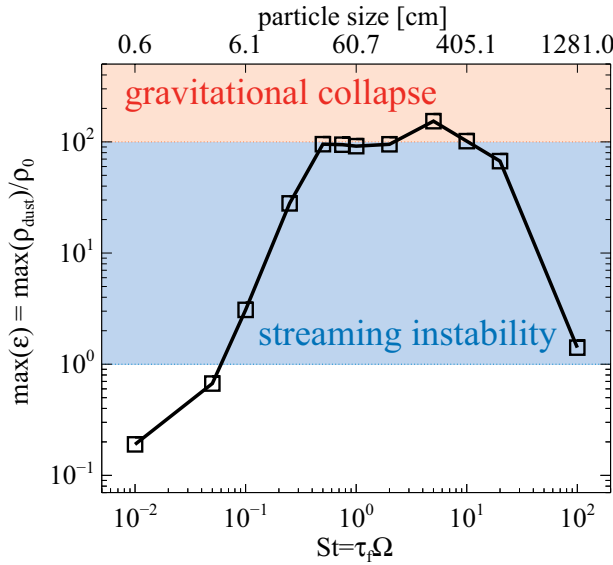


**Figure 3.** Shows the highest over-density that occurred for the specific particle size during the entire simulation. The upper labels correspond to particle sizes in a MMSN at 5 AU distance to the star using equations (3.2) and (3.3). The gravitational collapse regime starts at a dust-to-gas ratio of 100, according to equation (3.1). The streaming instability regime starts at  $\epsilon = 1$  (Johansen & Youdin 2007, Youdin & Johansen 2007). Meter-sized boulders reach the gravitational collapse regime, while decimeter-sized pebbles will trigger the streaming instability. All particle sizes were initialized with  $\epsilon_0 = 10^{-2}$ .

We can convert the dimensionless Stokes number  $St = \tau_f \Omega$  to a real particle size. The friction time  $\tau_f$  correlates to the particle radius  $a$  with

$$a = \frac{\tau_f^{(Ep)} \Omega \Sigma_{\text{gas}}}{\sqrt{2\pi} \rho_{\bullet}}, \tag{3.2}$$

for Epstein drag and

$$a = \left[ \frac{9\tau_f^{(St)} \Omega \mu H}{4\rho_{\bullet} \sigma_{\text{mol}}} \right]^2, \tag{3.3}$$

for Stokes drag (see supplementary info for Johansen *et al.* 2007). Here  $\Sigma_{\text{gas}}$  is the column density of the gas,  $\rho_{\bullet}$  the density of solid material,  $\mu = 3.9 \times 10^{-24}$  g is the mean molecular weight and  $\sigma_{\text{mol}} = 2 \times 10^{-15}$  cm<sup>2</sup> is the molecular cross section of molecular hydrogen (Nakagawa *et al.* 1986, Chapman & Cowling 1970). The Epstein regime applies, if the particle radius  $a$  does not exceed (9/4) (Weidenschilling 1977) of the gas mean free path

$$\lambda = \frac{\mu}{\rho_{\text{gas}} \sigma_{\text{mol}}} = \frac{\sqrt{2\pi} \mu H}{\Sigma_{\text{gas}} \sigma_{\text{mol}}}. \tag{3.4}$$

### 4. Summary

We performed numerical simulations of MRI-driven turbulence in shearing boxes, covering the parameter space for radial and azimuthal box sizes up to 21.12H. Further, we

followed the reaction of the dust particle density to the turbulence. Our major findings are

(a) Particles get trapped downstream of pressure bumps and build up over-densities. In our simulations, we see that the density of  $\sim 60$  cm sized icy boulders increases several thousand times over the equilibrium density, even without streaming instability and self-gravity of the particles. Sedimentation to the mid-plane leads to over-densities of around 40, while the contribution from the turbulence concentrates the boulders several hundred times. We reach dust-to-gas ratios of 50 to 100. These densities are of the order of the Roche density at 5 AU in a MMSN. To what degree these high dust-to-gas ratios disturb the axisymmetric pressure bumps that developed in the zonal flows has to be investigated in further studies with back-reaction to the gas.

(b) Particles of only a few centimeters in size (at 5 AU) in a MMSN,  $St = 0.1$ ) accumulate in over-densities that are increased by a factor of  $\sim 100$ , leading to a dust-to-gas ratio of 1 in the mid-plane, thus triggering the streaming instability. Without MRI and zonal flows  $St = 0.1$  particles do not clump strongly and cannot trigger the streaming instability (Johansen *et al.* 2009b).

This is the first work on the effect from large-scale zonal flows on dust particles in a MHD simulation. Dust gets trapped downstream of long-lived high-pressure regions and achieves over-densities that have the potential to generate streaming instability and to become gravitationally unstable. Planetesimal formation in large boxes will be further investigated in simulations with particle feedback on the gas and self-gravitating particles in a future study.

In the future we will focus on one model and study various initial dust-to-gas ratios and particle size distributions. We will probably use the already converged run  $L$  ( $5.28H \times 5.28H \times 2.64H$ ). This choice is also a trade-off between simulation box size and computational expense.

## References

- Balbus, S. A. & Hawley, J. F. 1991, *ApJ*, 376, 214  
 Balbus, S. A. & Hawley, J. F. 1998, *Reviews of Modern Physics*, 70, 1  
 Brandenburg, A., Nordlund, A., Stein, R. F., & Torkelsson, U. 1995, *ApJ*, 446, 741  
 Chapman, S. & Cowling, T. G. 1970, Cambridge: University Press, 1970, 3rd ed.  
 Dittrich, K., Klahr, H., & Johansen, A. 2013, *ApJ*, 763, 117  
 Flock, M., Dzyurkevich, N., Klahr, H., Turner, N. J., & Henning, T. 2011, *ApJ*, 735, 122  
 Fromang, S. & Stone, J. M. 2009, *A&A*, 507, 19  
 Johansen, A., Oishi, J. S., Mac Low, M.-M., *et al.* 2007, *Nature*, 448, 1022  
 Johansen, A. & Youdin, A. 2007, *ApJ*, 662, 627  
 Johansen, A. 2009, *IAU Symposium*, 259, 249  
 Johansen, A., Youdin, A., & Klahr, H. 2009, *ApJ*, 697, 1269  
 Johansen, A., Youdin, A., & Mac Low, M.-M. 2009, *ApJ*, 704, L75  
 Kopal, Z. 1989, *Astrophysics and Space Science Library*, 152  
 Lyra, W., Johansen, A., Klahr, H., & Piskunov, N. 2008, *A&A*, 479, 883  
 Nakagawa, Y., Sekiya, M., & Hayashi, C. 1986, *Icarus*, 67, 375  
 Pinilla, P., Birnstiel, T., Ricci, L., *et al.* 2012, *A&A*, 538, A114  
 Stone, J. M. & Gardiner, T. A. 2010, *ApJS*, 189, 142  
 Weidenschilling, S. J. 1977, *MNRAS*, 180, 57  
 Whipple, F. L. 1972, *From Plasma to Planet*, 211  
 Youdin, A. & Johansen, A. 2007, *ApJ*, 662, 613